BJP British Journal of Pharmacology

DOI:10.1111/bph.13055
www.brjpharmacol.org

RESEARCH PAPER

The fibrate gemfibrozil is a NO- and haem-independent activator of soluble guanylyl cyclase: *in vitro* studies

I G Sharina[1], M Sobolevsky[1], A Papakyriakou[2], N Rukoyatkina[3,4], G A Spyroulias[5], S Gambaryan[3,4] and E Martin[1]

[1]*Department of Internal Medicine, Division of Cardiology, UT Health Science Center at Houston, Medical School, Houston, TX, USA,* [2]*National Center for Scientific Research, Department of Physical Chemistry, Athens, Greece,* [3]*Institute of Clinical Biochemistry and Pathobiochemistry, University of Wuerzburg, Wuerzburg, Germany,* [4]*Sechenov Institute of Evolutionary Physiology and Biochemistry, Russian Academy of Sciences, Petersburg, Russia, and* [5]*Department of Pharmacy, University of Patras, Patras, Greece*

Correspondence
Emil Martin, Department of Internal Medicine, Division of Cardiology, UT Health Science Center at Houston, Medical School, 1941 East Road, Houston, TX 77054, USA. E-mail: emil.martin@uth.tmc.edu

Received
27 August 2014
Revised
3 November 2014
Accepted
11 December 2014

BACKGROUND AND PURPOSE

Fibrates are a class of drugs widely used to treat dyslipidaemias. They regulate lipid metabolism and act as PPARα agonists. Clinical trials demonstrate that besides changes in lipid profiles, fibrates decrease the incidence of cardiovascular events, with gemfibrozil exhibiting the most pronounced benefit. This study aims to characterize the effect of gemfibrozil on the activity and function of soluble guanylyl cyclase (sGC), the key mediator of NO signalling.

EXPERIMENTAL APPROACH

High-throughput screening of a drug library identified gemfibrozil as a direct sGC activator. Activation of sGC is unique to gemfibrozil and is not shared by other fibrates.

KEY RESULTS

Gemfibrozil activated purified sGC, induced endothelium-independent relaxation of aortic rings and inhibited platelet aggregation. Gemfibrozil-dependent activation was absent when the sGC haem domain was deleted, but was significantly enhanced when sGC haem was lacking or oxidized. Oxidation of sGC haem enhanced the vasoactive and anti-platelet effects of gemfibrozil. Gemfibrozil competed with the haem-independent sGC activators ataciguat and cinaciguat. Computational modelling predicted that gemfibrozil occupies the space of the haem group and interacts with residues crucial for haem stabilization. This is consistent with structure-activity data which revealed an absolute requirement for gemfibrozil's carboxyl group.

CONCLUSIONS AND IMPLICATIONS

These data suggest that in addition to altered lipid and lipoprotein state, the cardiovascular preventive benefits of gemfibrozil may derive from direct activation and protection of sGC function. A sGC-directed action may explain the more pronounced cardiovascular benefit of gemfibrozil observed over other fibrates and some of the described side effects of gemfibrozil.

Abbreviations

BAY41-2272, (3-(4-amino-5-cyclopropylpyrimidine-2-yl)-1-(2-fluorobenzyl)-1*H*-pyrazolo[3,4-b]pyridine); DEA-NO, diethylammonium (Z)-1-(N,N-diethylamino)diazen-1-ium-1,2-diolate; ODQ, 1H-[1,2,4]oxadiazolo[4,3-a]quinoxalin-1-one; sGC, soluble GC

Tables of Links

TARGETS	
Nuclear hormone receptors[a]	**Enzymes**[b]
PPARα	sGC

LIGANDS		
ADP	Ciprofibrate	IBMX
Ataciguat	Clofibrate	Nitric oxide (NO)
Bezafibrate	Fenofibrate	ODQ
Cinaciguat	Gemfibrozil	Protoporphyrin IX

These Tables list key protein targets and ligands in this article which are hyperlinked to corresponding entries in http://www.guidetopharmacology.org, the common portal for data from the IUPHAR/BPS Guide to PHARMACOLOGY (Pawson *et al.*, 2014) and are permanently archived in the Concise Guide to PHARMACOLOGY 2013/14 ([a,b]Alexander *et al.*, 2013a,b).

Introduction

Gemfibrozil is a member of the fibrate class of drugs that have been used for decades for the management of combined dyslipidaemia (Fruchart and Duriez, 2006). Fibrates were introduced in clinics in the early 1970s and are currently widely used for dyslipidaemic patients with diet-resistant hypertriglyceridaemia. Fibrates act as agonists for the transcription factor PPARα, which controls the expression of genes associated with lipid catabolism and metabolism of lipoproteins, resulting in stimulated cellular fatty acid uptakes, enhanced catabolism of triglyceride-rich particle and reduced secretion of very low-density lipoprotein (Staels *et al.*, 1998). Fibrates cause a substantial decrease in the level of plasma triglycerides, usually accompanied by a moderate decrease of low-density lipoprotein cholesterol and an increase in high-density lipoprotein cholesterol (Staels *et al.*, 1998). Additional effects on endothelial function, inflammation and vascular remodelling have also been reported (Chinetti-Gbaguidi *et al.*, 2005). Meta-analyses of clinical trials demonstrate that fibrates improve lipid profile and have an overall reduction in cardiovascular and coronary events (Jun *et al.*, 2010). While improved lipid profile is consistently observed in all fibrate studies, the extent of cardiovascular and coronary benefits is drug-specific. Clinical trials of gemfibrozil, such as the Helsinki Heart Study (Frick *et al.*, 1987) and VA-HIT (Rubins *et al.*, 1999), show the most pronounced cardiovascular preventive benefits and a decreased incidence of coronary events over other fibrates. We report here that at therapeutic concentrations gemfibrozil, but not other fibrates, acts as an activator of soluble GC (sGC).

sGC synthesizes the secondary messenger cGMP in response to NO stimulation. In the cardiovascular system, sGC regulates BP, platelet function, vascular plasticity and angiogenesis (Murad, 2006). Diminished sGC activity and expression exacerbate endothelial dysfunction, decrease vascular plasticity (Ruetten *et al.*, 1999; Kloss *et al.*, 2000) and contribute to the development of a wide array of cardiovascular disorders, including hypertension, coronary artery disease and atherosclerosis (Xu and Zou, 2009; Vita, 2011). Single nucleotide polymorphisms of human sGC loci are linked to increased risk of hypertension and coronary artery disease (Ehret *et al.*, 2011; Lu *et al.*, 2012). Familial studies in humans demonstrate that diminished sGC expression correlates with increased risk of myocardial infarctions (Erdmann *et al.*, 2013b), stenosis of carotid arteries or oesophageal achalasia (Herve *et al.*, 2014).

Not surprisingly, sGC is an active target for pharmacological intervention. Classical nitrovasodilators have been used to manage angina and heart failure long before it became clear that they act as NO-generating compounds. The interest in sGC as a drug target was substantially renewed because of the discovery of several NO-independent allosteric regulators of sGC. Some of these regulators are being developed for clinical applications. Recently, riociguat, a sGC stimulator, which moderately activates sGC, but significantly increases its affinity to NO (Stasch and Hobbs, 2009), has been approved as a new therapy for pulmonary hypertension (Stasch and Evgenov, 2013). Other compounds, such as ataciguat and cinaciguat, activate sGC by mimicking haem (Schmidt *et al.*, 2009). Cinaciguat is considered for treatment of heart failure (Zamani and Greenberg, 2013), although some side effects are yet to be resolved (Erdmann *et al.*, 2013a). The effects of both sGC stimulators and haem-independent activators are enhanced by cobinamides, which act independently of sGC haem and its haem-binding region (Sharina *et al.*, 2011a; Chrominski *et al.*, 2013).

Multiple modes of sGC stimulation and the structural diversity of existing sGC regulators suggest that some of the drugs currently used in clinical practice may inadvertently target sGC. In this study, we report that gemfibrozil is a haem-independent sGC activator with vasorelaxation and antiplatelet properties.

Methods

Recombinant human sGC enzyme

Full-length sGC was purified from Sf9 cells as described previously (Martin *et al.*, 2001). To generate truncated sGC variants, the open reading frames coding the residues 269–690 of the α subunit or the residues 200–619 of the β subunit were cloned into the transfer vector pBacPak9 (Clontech, Mountain View, CA, USA) to obtain the pBacPak-αΔ269 and the pBacPak-βΔ200 plasmids respectively. A hexahistidine tag was also inserted at the C-terminus of the αΔ269 variant by PCR mutagenesis. Using these plasmids and the linearized baculovirus DNA (BaculoGold from Pharmingen, San Diego, CA, USA), the baculoviruses expressing the truncated αΔ269 or

βΔ200 sGC were generated according to the manufacturer's protocol. To generate the full-length or truncated sGC variants, Sf9 cells were infected with the appropriate combination of baculovirus and, after 72 h, sGC enzyme was partially purified from the lysates using the anion exchange chromatography on HR16/50 DEAE-FF Sepharose column (GE Healthcare Bio-Sciences, Pittsburgh, PA, USA).

High-throughput screening sGC assay

The libraries were screened in 96-well plates as described previously (Sharina *et al.*, 2011a). In brief, 1 μL of 10 mM pharmacophore was delivered robotically into 30 μL reaction solution [40 mM triethanolamine (TEA), pH 7.4, 0.1 mM DTT, 0.2 mM $MgCl_2$] containing 0.1 μg of purified human recombinant sGC and 10 mU of inorganic pyrophosphatase. Synthesis of cGMP was initiated after 5 min by adding 10 μL of 400 μM Mg^{2+}-GTP. The reaction was stopped 15 min later by 60 μL of 0.5 M HCl and the amount of generated phosphate was determined colorimetrically at 630 nm 20 min after adding 100 μL of developing reagent [1.05% (w v^{-1}) ammonium molybdate, 1 M HCl, 0.034% (w v^{-1}) malachite green and 0.05% Tween 20]. sGC activities in the absence of additives (basal), in the presence of BAY41-2272 (5 μM) or 10 μM ODQ with 100 nM BAY58-2667 were used as positive controls. Positive samples were rescreened manually using the [α-^{32}P]GTP→[α-^{32}P]cGMP conversion assay. The pharmacophores displaying OD >0.1 AU above the level of basal activity were subjected to secondary screening.

Assay of sGC activity in vitro

Enzymatic activity was assayed using [α-^{32}P]GTP to [^{32}P] cGMP conversion assay (Schultz, 1974). sGC, 0.5 μg, in 25 mM TEA, pH 7.5, 1 mg·mL^{-1} BSA, 1 mM IBMX, 1 mM DTT, 1 mM cGMP, 3 mM $MgCl_2$, 0.05 mg·mL^{-1} creatine phosphokinase and 5 mM creatine phosphate was incubated with indicated concentrations of agonist(s) (gemfibrozil, ataciguat, cinaciguat or BAY41-2272) for 10 min at room temperature. After transferring the sample to 37°C, the reaction was initiated by 1 mM GTP/[α-^{32}P]GTP (~100 000 cpm). To measure NO-induced sGC activity, 10 ng of sGC were used and NO donor was supplied together with GTP. To deplete sGC of haem, purified sGC was incubated with 0.4% Tween 20 for 20 min at room temperature before adding it into the reaction mixture. For the experiments with ferric sGC, the enzyme was incubated for 20 min with 10 μM ODQ before it was used in the reaction. The reaction was stopped by zinc carbonate and processed following the protocol established previously (Schultz, 1974).

Aortic ring relaxation

Male Sprague Dawley rats (20 animals total; 14–16 weeks old, 300–350 g; Harlan Laboratories Inc, Indianapolis, IN, USA) were killed while under isoflurane anaesthesia and after thoracotomy, the descending thoracic aorta was dissected, cut into 3–5 mm long segments and mounted on a four-channel wire Myograph 610 (DMT, Copenhagen, Denmark) under 1.5 g of passive tension. For endothelium-denuded vessels, the endothelium was removed by gently rubbing the vessel interior with a toothpick with a wet cotton swab. Removal of the endothelium was confirmed by the absence of ACh relaxation in vascular strips pre-contracted with submaximal concentrations of phenylephrine (Phe). The rings were equilibrated for 80 min in Krebs-Henseleit solution pH 7.4, oxygenated with carbogen (95% O_2, 5% CO_2) with at least three buffer changes every 20 min. All force measurements were recorded using Powerlab 400^{TM} data acquisition system and LabChart software (ADInstruments, Colorado Springs, CO, USA). After equilibration the rings were pre-contracted with 60 mM K^+ to determine the maximal contractile response, the buffer was then replaced and the rings were titrated with 100–300 nM Phe to achieve submaximal contraction of ~4.5–5 g of tension. After stabilization, the agonists (gemfibrozil or gemfibrozil analogues) were added cumulatively and changes in isometric tension were recorded. In some experiments, the rings were pretreated with 10 μM ODQ or 0.1 μM BAY41-2272. All studies involving animals are reported in accordance with the ARRIVE guidelines for reporting experiments involving animals (Kilkenny *et al.*, 2010; McGrath *et al.*, 2010).

Preparation of washed human platelets

Human platelets were prepared and used as previously reported (Gambaryan *et al.*, 2010) with small modifications. Blood was collected into one-seventh volume of anticoagulant citrate dextrose solution (12 mM citric acid, 15 mM sodium citrate, 25 mM dextrose and 2 μM EGTA, final concentrations). Platelet-rich plasma (PRP) was obtained by 5 min centrifugation at 330× *g*. To reduce leukocyte contamination, PRP was diluted 1:1 with PBS and centrifuged at 240× *g* for 10 min. Subsequently, the supernatant was centrifuged for 10 min at 430× *g*, then the platelets were washed once in citrate glucose saline buffer (120 mM sodium chloride, 12.9 mM trisodium citrate, 30 mM D-glucose, pH 6.5) and resuspended in HEPES buffer (150 mM sodium chloride, 5 mM potassium chloride, 1 mM magnesium chloride, 10 mM D-glucose, 10 mM HEPES, pH 7.4). After 15 min rest in a 37°C water bath, washed platelets (WP) were used for experiments.

Western blot analysis

One hundred microlitres of WP (1×10^8 mL^{-1}) were incubated at 37°C for 1 min with vehicle (resuspension HEPES buffer), 10 or 100 μM NO donor DEA-NO or with 10 or 100 μM gemfibrozil for 5 min. In experiments with ODQ, platelets were pre-incubated for 1 min with 10 μM ODQ before the addition of the vehicle (HEPES buffer), DEA-NO or gemfibrozil. At the end of the incubation, the reactions were stopped by adding an equal volume of 2× Laemmli buffer (200 mM Tris-HCl, pH 6.7, 20% glycerol, 4% SDS and 10% 2-mercaptoethanol) and boiling at 97°C for 5 min. Platelet lysates were separated by SDS-PAGE, transferred to nitrocellulose membranes and the membranes were incubated with anti-Phospho-VASP^{Ser239} (Nanotools, Teningen, Germany) or anti-β-actin (Cell Signaling, Frankfurt am Main, Germany) antibodies overnight at 4°C. To visualize the signal, goat anti-rabbit or anti-mouse IgG conjugated with HRP were used as secondary antibodies, followed by ECL detection.

Platelet aggregation

Platelet aggregation was analysed in diluted PRP by recording the intensity of low angle light scattering using the method

described in detail previously (Mindukshev *et al.*, 2011). All experiments were performed in 6 mL of modified HEPES buffer (pH 7.4, osmolarity 302 mOsm, containing 140 mM NaCl, 10 mM HEPES, 10 mM $NaHCO_3$, 2 mM KCl, 1 mM $MgCl_2$, 2 mM $CaCl_2$, 5.5 mM D-glucose). An appropriate amount of PRP was added to the buffer to achieve a density of 10 000 platelets μL^{-1}. After 2 min of establishing a constant basal signal, platelets were pre-incubated with the indicated concentrations of gemfibrozil, SNP, BAY 41–2272 alone or in combination with ODQ (which was added 1 min before) for 5 min. Aggregation was initiated by 0.1 μM ADP and the signal was recorded for an additional 10 min. The mean light scatter signal in control experiments without stimulation was expressed as 100% aggregation.

Molecular modelling of human β1 H-NOX complex with gemfibrozil

Human *β1* H-NOX domain (*h*HNOX) was modelled based on the crystal structure of the homologous *Ns*HNOX protein from *Nostoc sp* (PDB ID: 3L6J; Martin *et al.*, 2010). Briefly, the crystallographic coordinates were employed as a template for the production of the *h*HNOX domain using the programme Modeller v9 (Fiser and Sali, 2003). The model with the lowest target function was selected among 50 models and its quality was assessed using the Structural Analysis and Verification Server (see Supplemental Information for more details). Subsequently, the model of *h*HNOX was superimposed with the template X-ray structure so as to transfer the ligand at its crystallographic pose. To relax the resulting *h*HNOX complex with cinaciguat from steric classes, the model was subjected to energy minimization using AMBER v12 (Case *et al.*, 2005). The ligand-free, energy minimized model of the *h*HNOX domain was employed for docking of the inhibitors using AutoDock v4 (The Scripps Research Institute, San Diego, CA, USA; Huey *et al.*, 2007).

Statistical analysis

Non-linear regression, calculation of EC_{50} and statistical analysis were performed using GraphPad Prism 5.1 (GraphPad Software, La Jolla, CA, USA). One-way ANOVA, followed by Turkey's *post hoc* test was used for multiple comparisons. Two-way ANOVA followed by Bonferroni's *post hoc* test was used for comparison of the dose-response curves. $P < 0.05$ was considered significant. Results are expressed as mean ± SEM. The EC_{50} values are expressed as means with 95% confidence interval shown in parentheses.

Materials

IBMX, phosphocreatine, creatine kinase, GTP, pyrophosphatase, ammonium molybdate, malachite green, Tween 20 and gemfibrozil were obtained from Sigma-Aldrich (St Louis, MO, USA). Fibrates and gemfibrozil-like compounds used in structure-activity studies (Supporting Information Table S1) were also from Sigma-Aldrich. 2-(N,N-diethylamino)-diazenolate-2-oxide [diethylammonium salt] (DEA-NO), ataciguat, cinaciguat, BAY41-2272 and ODQ were obtained from Enzo Life Sciences (Farmingdale, NY, USA).

Study approval

Blood was obtained from healthy volunteers according to institutional guidelines and the Declaration of Helsinki. The studies with human platelets were performed at the University of Würzburg according to the guidelines of the ethics committee of the University of Würzburg (Studies No. 67/92 and 114/04). The studies of isolated rat aortic rings were performed in accordance to the guidelines of the Animal Welfare Committee of the University of Texas Health Science Center (protocol AWC 12–089).

Results

Identification of gemfibrozil as sGC activator

We have previously developed a high-throughput *in vitro* screening for selection of sGC activating compounds (Sharina *et al.*, 2011a). We have reported that screening of a small library containing 1120 'off-patent' drugs (Prestwick Chemical Library, ChemBridge Corporation, San Diego, CA, USA) and selected vitamins and pro-vitamins identified two sGC-activating compounds. The effect of vitamin B12 precursor dicyanocobinamide on sGC activity was already reported (Sharina *et al.*, 2011a). In addition, gemfibrozil (Figure 1A) was identified as a potential sGC activator. Because gemfibrozil is a member the fibrate class of drugs, we tested all structurally related fibrates. We determined that none of them was capable to activate sGC (Figure 1A). This indicates that among fibrates, sGC activation is a feature specific only to gemfibrozil. Gemfibrozil-dependent activation of sGC was observed over a broad range of concentrations (Figure 1B), with an apparent EC_{50} of 94 [75–117] μM and a Hill slope coefficient of 1.96. BAY41-2272, the structural precursor of sGC stimulator riociguat, additively enhanced the effect of gemfibrozil and decreased the EC_{50} to 48 [37–67] μM and the Hill coefficient to 1.34. Such additive effect strongly suggests non-overlapping binding sites for BAY41-2272 and gemfibrozil. Moreover, the EC_{50} for NO donor DEA-NO only marginally changed in the presence of gemfibrozil (Figure 1C), although the maximal NO activation was diminished. These analyses indicate that gemfibrozil's mechanism of action is different from that of described sGC stimulators.

Gemfibrozil-dependent activation requires the haem-binding domain of sGC

To further understand the mechanism of action of gemfibrozil, we used the α1 splice isoform D, which lacks the N-terminal 239 residues of the α1 subunit (Sharina *et al.*, 2008; 2011b; Martin *et al.*, 2014) and/or truncated versions of sGC lacking the N-terminal 200 residues of the β1 subunit (Figure 2A). Similar to wild-type sGC, all expressed truncated sGC variants (Figure 2B) possessed cGMP-forming activity and were more active in the presence of Mn^{2+}. These properties argue for functional catalytic domains (Figure 2C) in these truncated sGC. However, only sGC variants containing intact β1 HNOX domain were activated by gemfibrozil. These data indicate that the haem-binding domain is necessary for gemfibrozil-dependent activation of sGC.

Gemfibrozil-dependent activation is enhanced by depletion and oxidation of sGC haem

Heme plays a crucial role in the mechanism of action for most pharmacological sGC regulators. Therefore, we evalu-

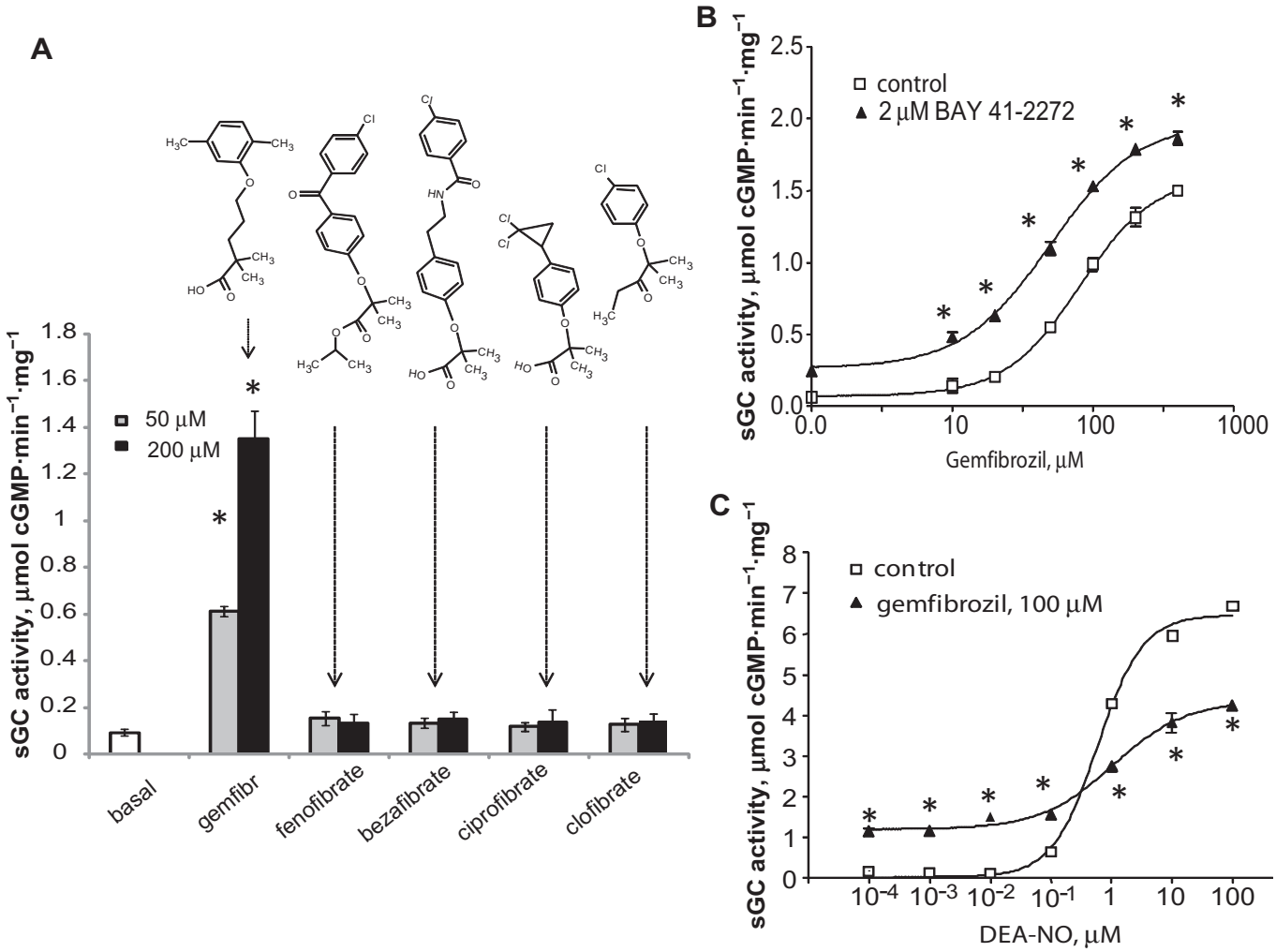

Figure 1

Gemfibrozil-dependent activation of sGC and its effect of NO stimulation. (A) sGC is activated by gemfibrozil, but not by other fibrates. Values are mean ± SEM (n = 9). *P < 0.05 versus control (basal activity). (B) Activity of purified sGC in the presence of indicated concentrations of gemfibrozil. Values are mean ± SEM (n = 5). *P < 0.05 versus control. (C) Gemfibrozil blunts maximal response to NO without affecting the EC_{50} value. Values are mean ± SEM (n = 6). *P < 0.05 versus control.

ated how depletion or oxidation of sGC haem affects gemfibrozil-dependent activation. To facilitate haem depletion, sGC was pretreated with 0.4% Tween 20 prior to the assay (Foerster *et al.*, 1996; Martin *et al.*, 2003). As expected, sGC with depleted haem exhibited weaker activation by NO, but was robustly activated by protoporphyrin IX (PPIX) and the haem-independent sGC activators ataciguat and cinaciguat (Figure 3B). ODQ, a haem oxidizing compound with high affinity for sGC, was used to oxidize sGC haem. In line with previous publications, ODQ-induced haem oxidation decreased the activation by DEA-NO, enhanced the effect of ataciguat and cinaciguat and had little effect on sGC activation by PPIX. Gemfibrozil-dependent activation of sGC was enhanced both by haem depletion and by haem oxidation (Figure 3B), a pattern that is characteristic for haem-mimicking sGC activators ataciguat and cinaciguat (Schmidt *et al.*, 2009).

Gemfibrozil competes with haem-independent sGC activators

Next, we evaluated how gemfibrozil interacts with other known haem-independent sGC activators, ataciguat and cinaciguat. We found that high concentrations of gemfibrozil decreased maximal activation by ataciguat and cinaciguat (Figure 3C and D). Moreover, high concentrations of gemfibrozil almost doubled the apparent EC_{50} for ataciguat, 1.1 [0.9–1.3] µM versus 1.7 [1.1–3.1] µM, and for cinaciguat, 14 [12–16] nM versus 26 [22–32] nM. These effects are consistent with competition for overlapping sites.

Gemfibrozil has antiplatelet properties

We investigated if gemfibrozil-dependent activation of purified sGC translates into functional effects *ex vivo*. First, we tested if gemfibrozil modulates sGC-dependent

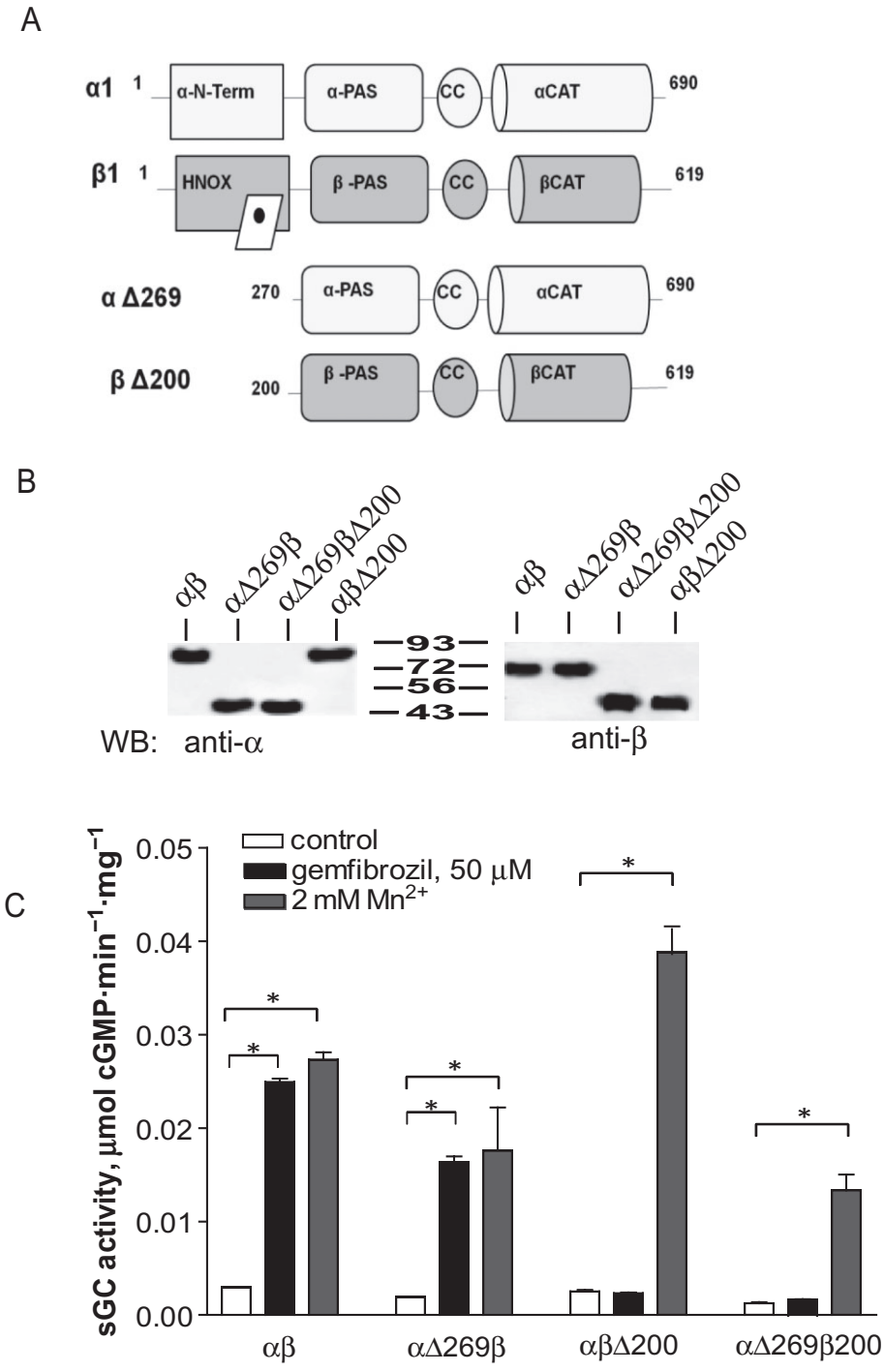

Figure 2

Gemfibrozil targets the haem-binding domain. (A) Schematic representation of domain structure of full-length α1, β1 and truncated αΔ269, βΔ200 sGC variants. CAT, GC catalytic domains; CC, coil-coil elements and Per/Arnt/Sim –like (PAS) domain are involved in dimerization; haem-NO/oxygen binding domain of the β subunit (HNOXβ) binds haem; α NH2-dom- – amino-terminal domain of the α subunit. (B) Representative Western blotting of Sf9 lysates expressing α1β1, α1βΔ200, αΔ269β1 and αΔ260βΔ200. (C) Gemfibrozil activates only sGC variants with intact β HNOX domain. cGMP-forming activity in lysates of Sf9cells expressing indicated sGC variants was tested without additives (control), in the presence of 50 μM gemfibrozil or 2 mM Mn^{2+}. Values are mean ± SEM ($n = 6$) *$P < 0.05$.

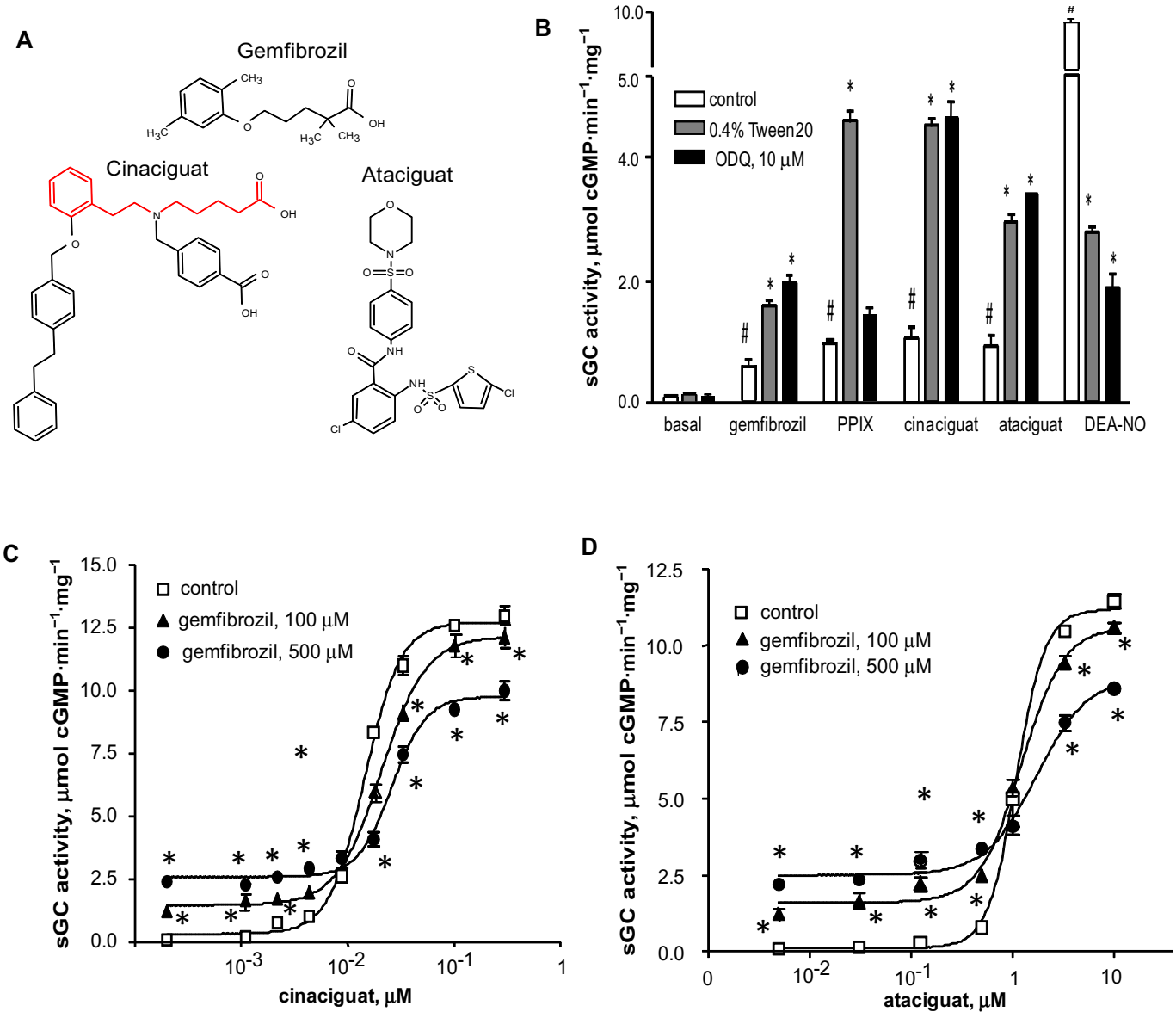

Figure 3

Gemfibrozil competes with haem-independent sGC activators. (A) Structures of gemfibrozil and haem-mimicking ataciguat and cinaciguat. (B) Effect of sGC haem depletion (0.4% Tween 20) or oxidation (10 µM ODQ) on sGC activation by 50 µM gemfibrozil, 25 µM protoporphyrin IX (PPIX), 1 µM cinaciguat, 10 µM ataciguat or 10 µM DEA-NO. Values are mean ± SEM from two independent experiments performed in triplicate. *P < 0.05 vs. control; #P < 0.05 vs. basal control. (C and D) Activity of human sGC treated with cinaciguat (C) or ataciguat (D) in the presence of 0, 100 and 500 µM gemfibrozil. Values are mean ± SEM (n = 6). *P < 0.05 versus control.

effects on platelets signalling and function. Phosphorylation of vasodilator-stimulated phosphoprotein VASP at Ser 239 is a specific and sensitive marker for increased cGMP-dependent kinase activity. Therefore, we evaluated the level of pVASP^{Ser239} in isolated platelets treated with gemfibrozil. As demonstrated in Figure 4, the level of pVASP^{Ser239} increased in response to gemfibrozil. Moreover, consistent with data on purified sGC (Figure 3), platelets pretreated with ODQ exhibited a stronger response to gemfibrozil and a substantial increase of pVASP^{Ser239}.

NO-dependent sGC activation inhibits platelet aggregation. We evaluated if sGC activation by gemfibrozil has similar effects on platelets. In agreement with VASP phosphorylation data, gemfibrozil-treated platelets exhibited diminished aggregation in response to 0.1 µM ADP. Moreover, platelets pretreated with ODQ displayed a more pronounced antiplatelet effect of gemfibrozil (Figure 5).

Gemfibrozil is a vasoactive agent

Because activation of vascular sGC leads to relaxation of blood vessels, we tested if gemfibrozil has any vasoactive effects. Gemfibrozil caused dose-dependent relaxation of rat aortic rings pre-contracted with Phe (Figure 6A) with an esti-

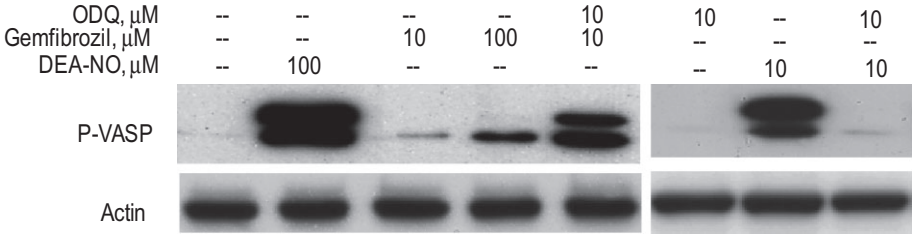

Figure 4

Gemfibrozil induces phosphorylation of VASP protein in platelets. One hundred microlitres of washed human platelets (1×10^8 mL^{-1}) were stimulated with the indicated concentrations of DEA-NO for 1 min, gemfibrozil for 5 min or pre-incubated for 1 min with ODQ and processed for Western blot analysis with Phospho-VASP^{Ser239} or β-actin (loading control) antibodies. Shown is one representative Western blot out of four experiments with similar results.

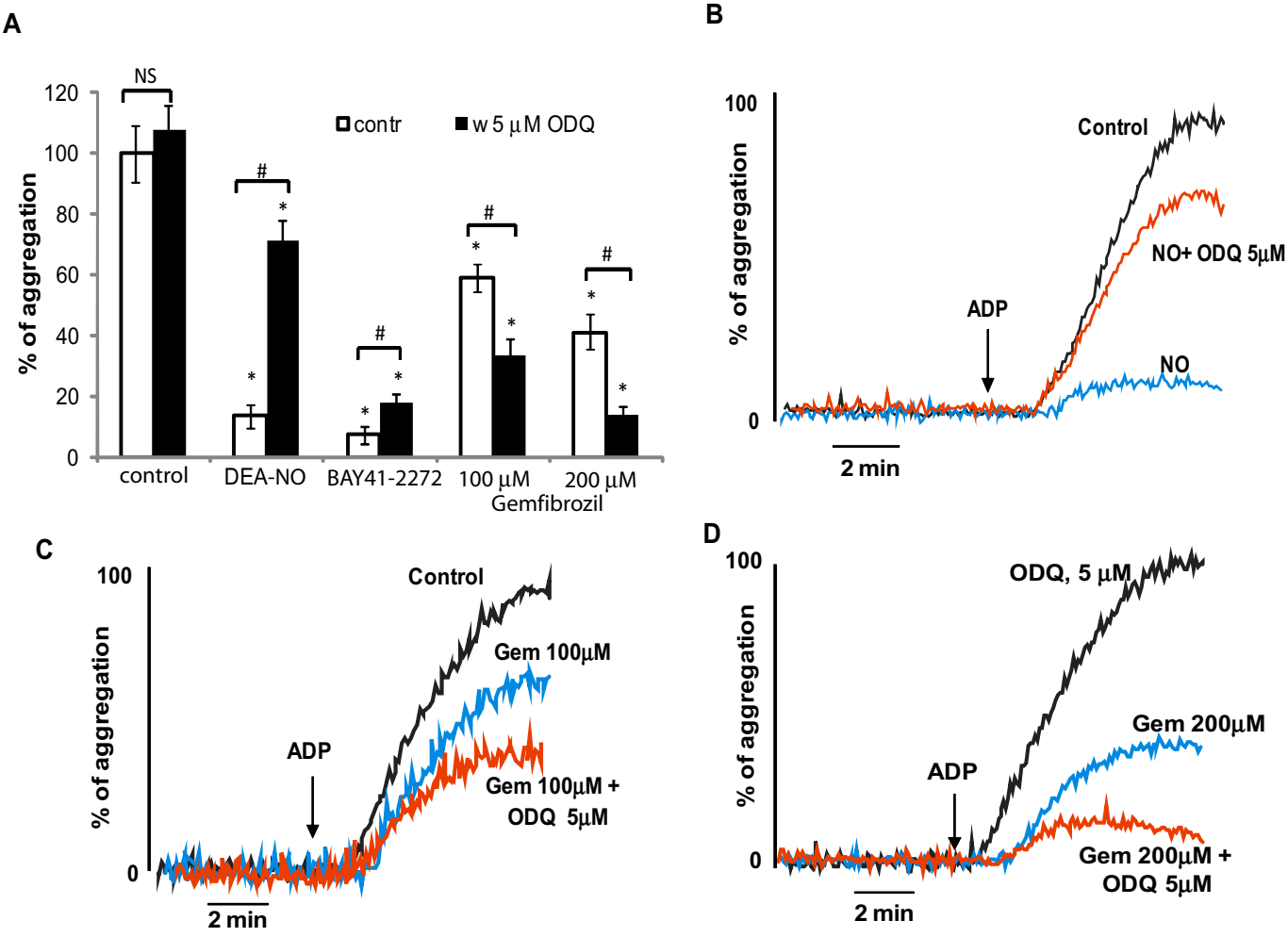

Figure 5

Gemfibrozil inhibits ADP-induced platelet aggregation. (A) Platelet aggregation induced by 0.1 μM ADP and light scatter signal was recorded as described in the Methods section. PRP was pre-incubated for 5 min before stimulation with ADP with vehicle (control) or 1 μM NO donor, 2 μM BAY41-2272; 100 μM or 200 μM gemfibrozil. In all experiments, ODQ was added 1 min before gemfibrozil, NO donor or BAY 41–2271. The mean light scatter signal in control experiments without stimulation is expressed as 100%. Data are expressed as a % of mean aggregation of platelets treated with control vehicle. Each value represents the mean ± SEM ($n = 5$). *$P < 0.05$ versus untreated control; #$P < 0.05$. (B–D) Representative traces depicting aggregation dynamics of control or ODQ-treated platelets in the presence of 1 μM NO (B), 100 μM (C) or 200 μM (D) gemfibrozil.

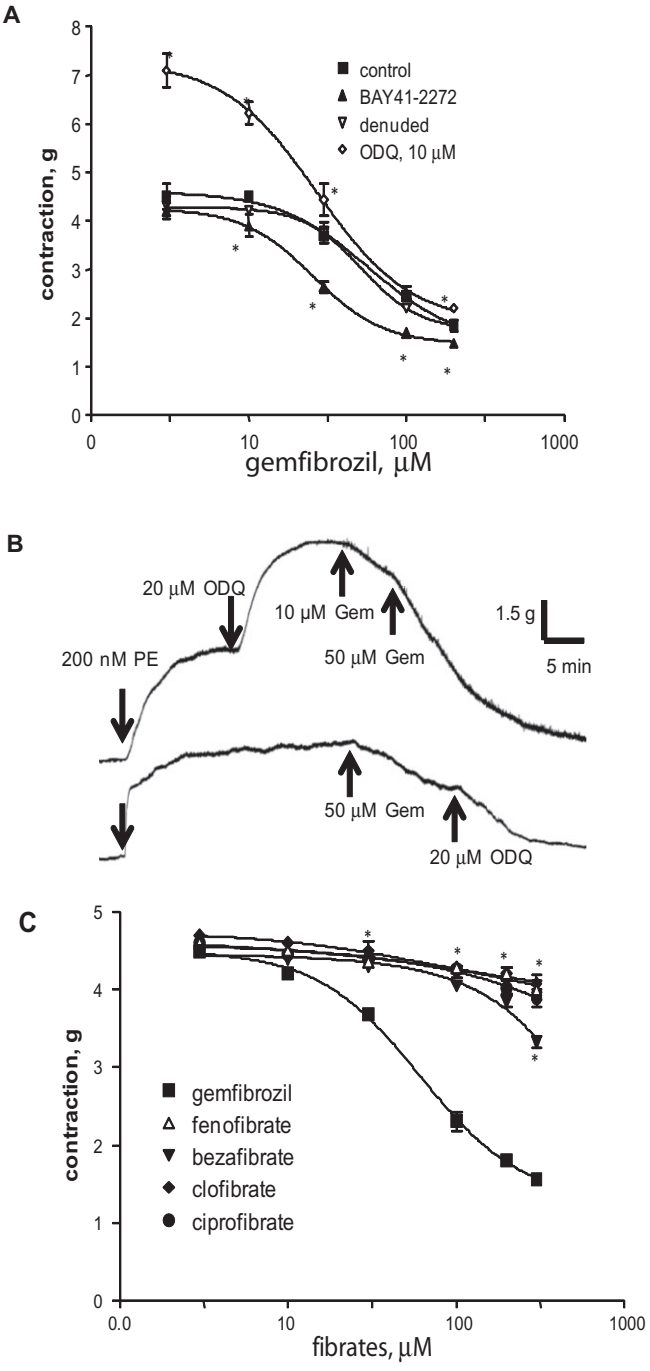

Figure 6

Vasoactive effect of gemfibrozil and other fibrates. (A) Relaxation of pre-constricted rat aortic rings with denuded or intact endothelium in response to different concentrations of gemfibrozil alone or in the presence of 100 nM BAY41-2272 or 10 μM ODQ. Data are mean ± SEM (n = 5), *P < 0.05 versus control. (B) Representative wire myograph traces showing synergistic vasodilatation by the combination of gemfibrozil and ODQ. Note that in the presence of gemfibrozil ODQ induces vessel relaxation. PE, phenylephrine; Gem, gemfibrozil. (C) Relaxation of aortic rings in response to different concentrations of fibrates. Values are mean ± SEM (n = 5). *P < 0.05 versus gemfibrozil.

mated EC_{50} of ~61 [37–100] μM. Consistent with direct sGC activation, denudation of endothelium did not alter gemfibrozil-dependent vasorelaxation (EC_{50} ~56 [33–81] μM). In agreement with the results obtained on purified sGC, BAY41-2272 and ODQ enhanced gemfibrozil-induced vasodilatation and improved gemfibrozil's EC_{50} to 25 [10–52] and 27 [9–61] μM respectively. It should be noted that, contrary to its effect on control naïve vessel, ODQ induced vasodilatation in vessels exposed to gemfibrozil (Figure 6B). None of the other tested fibrates had any vasoactive effects (Figure 6C).

Structure-activity relationship studies

To gain insight into the mechanism of gemfibrozil's action, we performed structure-activity analysis. Gemfibrozil features a 2,2-dimethylpentanoic acid connected to a dimethylphenoxy moiety. Therefore, we evaluated the contribution of the straight-chain alkyl carboxylic acid and the substituted phenoxy group. Because none of the other fibrates activated sGC (Figure 1), additional compounds containing one or both analysed groups were tested for sGC activation. Structures and complete chemical names of tested compounds are listed in Supporting Information Table S1. As shown in Figure 7, only two tested compounds, **1** and **3**, exhibited measurable sGC activation at 100 μM. Similar to gemfibrozil, both compounds contain a dimethylpentanoic acid connected to a substituted phenoxy group. Compound **2**, which contains a carboxylic ester, had no effect on sGC, underlining the importance of the carboxyl moiety. However, free alkyl carboxylic acids (compounds **11–14**) did not stimulate sGC. The compounds with substituted phenoxy group without the benefit of dimethylpentanoic acid also did not have any effects on sGC activity.

Vasoactivity data showed similar results. As demonstrated in Figure 8, compound **3** caused relaxation (EC_{50} ~108 [36–326 μM]), but was less potent than gemfibrozil (EC_{50} ~61 [37–100] μM), compound **1** was a stronger vasorelaxant than gemfibrozil with an EC_{50} of ~20 [10–36] μM, while compound **2** exhibited no vasoactive effects.

Molecular docking of gemfibrozil in HNOX domain

To evaluate the possible arrangement of gemfibrozil within the space of the haem-binding domain, we derived a model of *h*HNOX domain (Supporting Information Fig. S1) based on the crystal structure of *Ns*HNOX from *Nostoc sp*, which share 35% sequence identity with sGC (Ma *et al.*, 2007). The X-ray structures of *Ns*HNOX with both haem and cinaciguat ligand have been determined previously (Ma *et al.*, 2007; Martin *et al.*, 2010). Initially, we performed docking of cinaciguat using the energy-minimized model of *h*HNOX. The quality assessment of the derived model of NOX is shown in Supporting Information Fig. S2. AutoDock successfully identified the crystallographic configuration of cinaciguat, both as the top-ranked solution (mean free energy of binding ΔG = –13.8 Kcal·mol^{-1}) and as the most populated conformational cluster (34 out of 100 poses). The lowest-energy conformation of cinaciguat was within only 1.3 Å atomic root mean square deviation from the X-ray structure (Figure 9A). Molecular docking of gemfibrozil within the haem-binding domain of

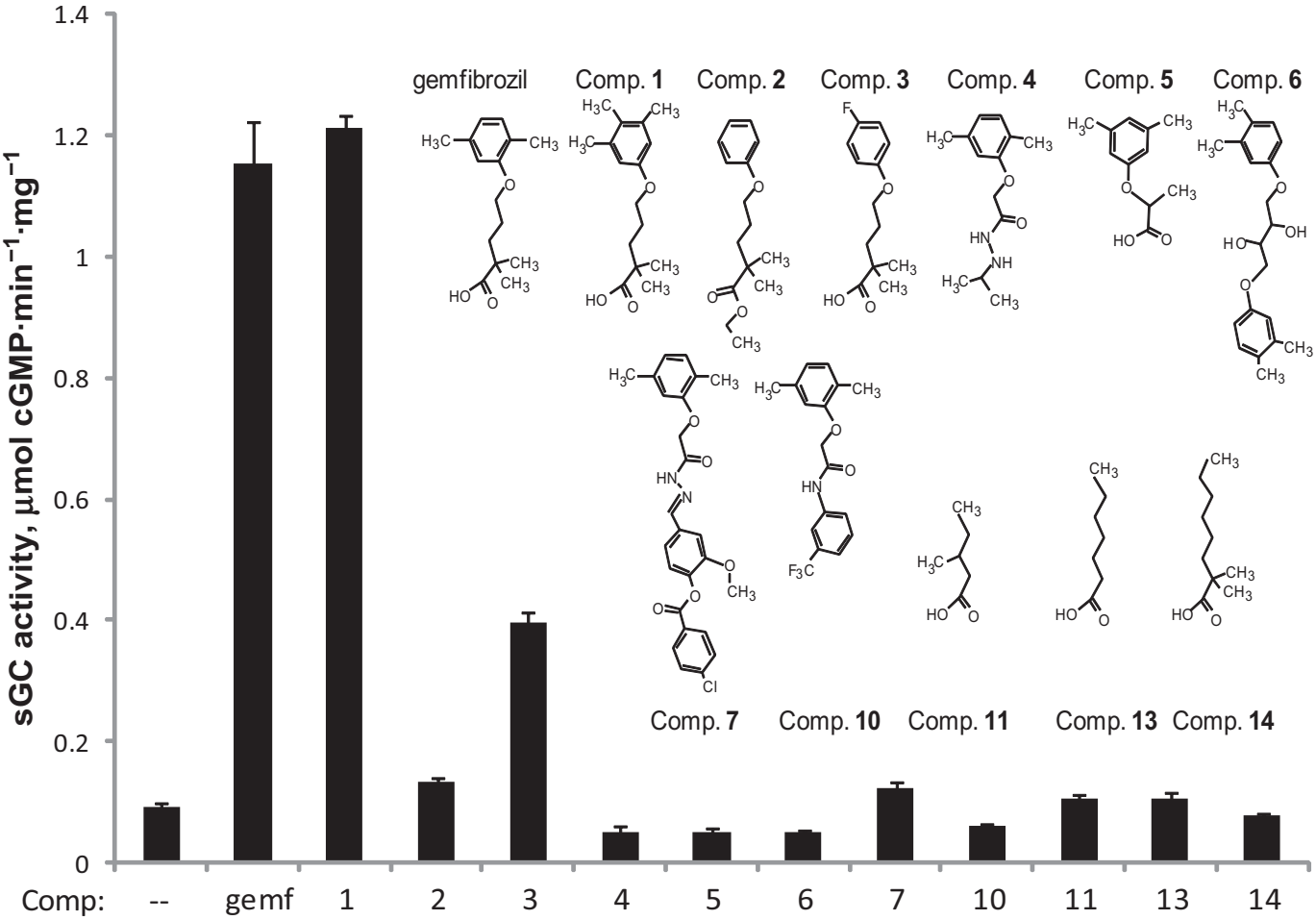

Figure 7

Structure-activity studies. Activity of purified sGC was determined in the presence of 100 µM gemfibrozil or tested compounds containing the phenoxy or alkyl carboxyl moieties. *Inset:* structures of tested compounds. Data are expressed as fold activation over basal sGC activity (control) – 0.075 µmol·min^{-1}·mg^{-1}. Values are mean ± SEM (n = 6). *P < 0.05 versus control. Gemf, gemfibrozil; comp, compound.

*h*HNOX model revealed two major conformational clusters (see Supplemental Information for more details). The top-ranked one (61% population) was the lowest-energy cluster with mean free energy of binding ΔG = –8.0 Kcal·mol^{-1}, whereas the second cluster (21% population) had a mean ΔG = –7.2 Kcal·mol^{-1}. Interestingly, the two lowest-energy poses from two distinct clusters are non-overlapping. Therefore, two gemfibrozil molecules can both fit inside the haem-binding site of *h*HNOX (Figure 9B).

Discussion and conclusions

Gemfibrozil belongs to the fibrate class of lipid-modifying agents, which function as PPARα agonists and are used to treat dyslipidaemias. In this report, we demonstrate that gemfibrozil also directly activates sGC, a property that is not shared by other fibrates.

Soluble GC is strongly activated by NO binding to ferrous haem located in the HNOX domain of the β sGC subunit. Allosteric sGC stimulators, such as YC-1, BAY41-2272 or riociguat, enhance sensitivity to NO (Stasch and Hobbs, 2009). Although the binding site for these stimulators is not determined, it is clear that they are effective only with ferrous sGC haem (Martin *et al.*, 2001). On the contrary, haem-independent activators cinaciguat or ataciguat are more potent when sGC haem is lost or oxidized (Schmidt *et al.*, 2009). Crystallographic studies demonstrate that cinaciguat occupies the same space as sGC haem (Martin *et al.*, 2010). Despite the differences in structure and mechanisms of action, all these sGC regulators target, or at least require, the haem-binding domain. To date, only cobinamides seems to regulate sGC through an allosteric mechanism that does not require haem domain (Sharina *et al.*, 2011a).

Mapping studies performed in this report demonstrate that intact HNOX domain is required for activation of sGC by gemfibrozil. Gemfibrozil is not an NO generator as it does not have NO moieties. Neither is gemfibrozil a sGC stimulator. We show that gemfibrozil and BAY41-2272 additively affect sGC activity, suggesting non-competing actions. Most importantly, gemfibrozil does not sensitize sGC to low concentrations of NO, a feature characteristic to sGC stimulators. On

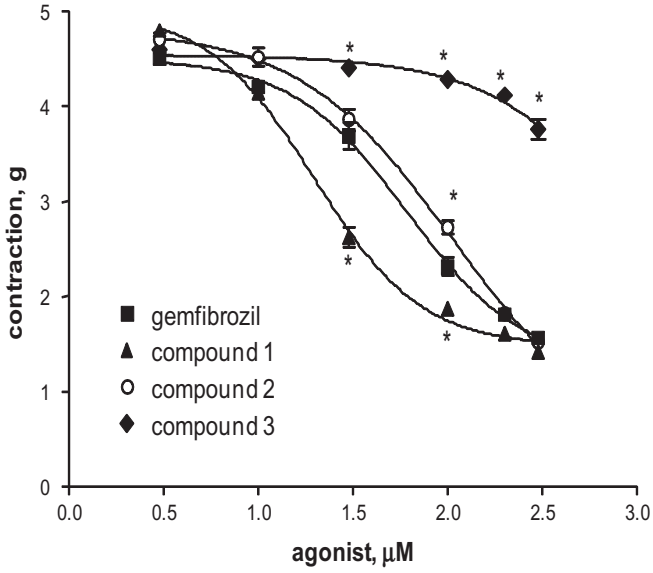

Figure 8

Vasoactive effects of gemfibrozil-like compounds. Relaxation of pre-contracted rat aortic rings in response to different concentration of gemfibrozil-like compounds. Values are mean ± SEM (n = 5). *P < 0.05 versus gemfibrozil.

the contrary, gemfibrozil diminishes maximal NO activation of sGC. Moreover, gemfibrozil-dependent activation is enhanced when sGC haem is oxidized or absent. This suggests a mechanism of action similar to haem-mimicking sGC activators. This conclusion is directly confirmed by competition studies. It should be noted that although gemfibrozil competes both with cinaciguat and ataciguat, it is a less potent sGC regulator. However, excess gemfibrozil reduces the extent of sGC activation by cinaciguat and ataciguat and increases their EC_{50}, behaving like a partial agonist. Together, these observations led us to conclude that gemfibrozil is an NO- and haem-independent sGC activator.

Structure-activity studies presented in this report were based on the concept that gemfibrozil consists of a substituted phenoxy group connected to a modified pentanoic acid. Testing sGC activation by a number of commercially available compounds that contain one or both of these groups provided insight into gemfibrozil's moieties crucial for sGC activation. None of the compounds containing only the phenoxy moiety activated sGC. Similarly, none of the free straight-chain alkyl carboxylic acids had any stimulating effects on sGC. Only molecules containing both moieties, such as compound **1** and **3**, had any effect on sGC activity. Activation by compound **1** and **3** suggests that the phenoxy moiety tolerate some minor modification without detrimental effects on sGC activation. In fact, compound **1**, which appears to have the same sGC activation potency as gemfibrozil, is a better vasorelaxing agent, probably because of better membrane permeability. Furthermore, compound **2**, carrying an ethyl pentanoate ester instead of pentanoic acid, does not activate sGC. This clearly indicates that the intact carboxyl group is crucial for gemfibrozil's action. The requirement for an intact –COOH is shared between gemfibrozil and

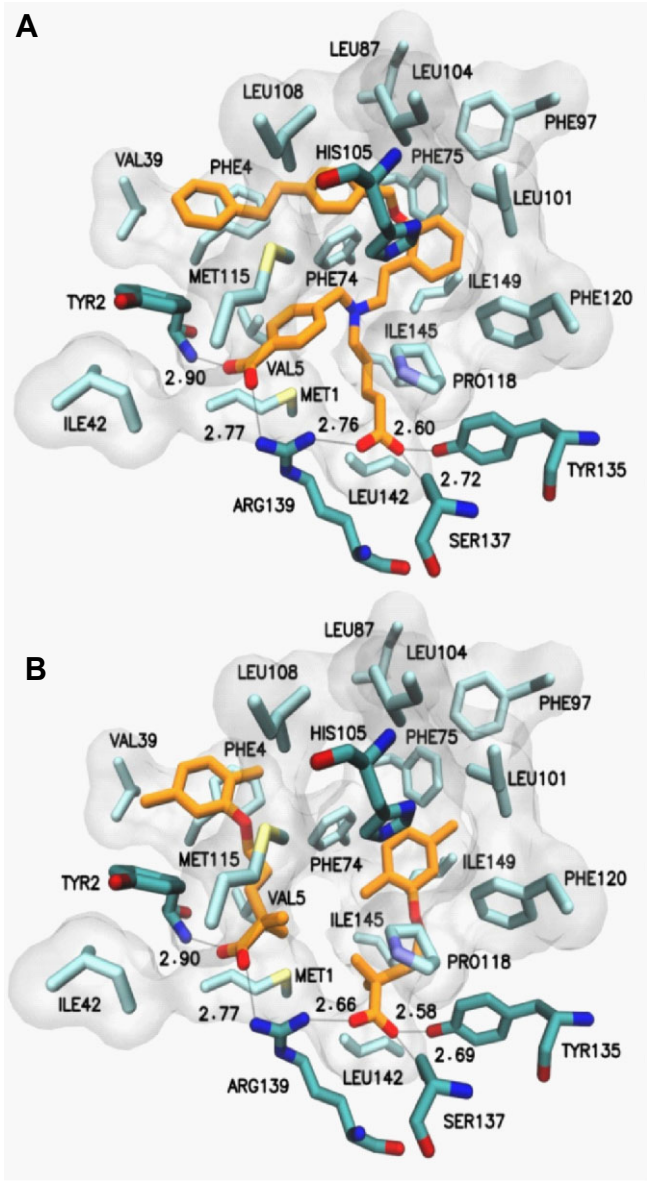

Figure 9

Molecular modelling of gemfibrozil binding site to HNOX domain. Close-up view of the human HNOX haem-binding pocket with bound cinaciguat (A) or two distinct molecules of gemfibrozil (B). The ligands are shown with orange carbon atoms and the HNOX residues in cyan. His105 and the hydrogen-bonding interacting residues Tyr2, Tyr135, Ser137 and Arg139 are highlighted. The hydrophobic side-chain atoms of the residues that interact with cinaciguat are shown in light cyan along with their van der Waals surface representation.

cinaciguat, which have some common structural features (red portion of cinaciguat in Figure 1A). The lack of sGC activation by compound **5**, which has a short alkyl chain, suggests that the chain length in the carboxylic acid is an important structural parameter that influences the potency of sGC activation. Additional studies will have to be performed to determine the optimal chain length.

Molecular modelling suggests that gemfibrozil may occupy the space reserved for the haem group, with two possible

orientations within the haem-binding cavity of *h*HNOX. Moreover, these two distinct clusters are non-overlapping, suggesting that two gemfibrozil molecules can both fit inside the haem-binding site of *h*HNOX. It should be noted that the fitting of the dose-activation curve has a Hill coefficient of 1.96, which may indirectly support cooperative binding of two gemfibrozil molecules. The top-ranked conformation of gemfibrozil displays hydrogen bonds between its carboxylate group, the backbone NH of Tyr2 and the guanidinium group of Arg139, while the second gemfibrozil pose shows its carboxylic acid to be hydrogen bonded to the YxSxR motif residues Tyr135, Ser137 and Arg139. These are the same residues that were shown to be crucial for interaction with and stabilization of haem propionates and carboxyl moieties of cinaciguat (Schmidt *et al.*, 2004; Ma *et al.*, 2007; Martin *et al.*, 2010). The dimethylphenoxy groups of gemfibrozil display extensive hydrophobic interactions with Val39, Phe4, Leu108, Ile149, Phe75, Leu101, Phe120 and Ile145 of *h*HNOX by occupying similar sites with the lipophilic moieties of cinaciguat. Consequently, the two predicted bound conformations of gemfibrozil could mimic the binding mode of the trifurcated cinaciguat ligand (Figure 9B), which occupies the haem cavity and has carboxylate groups at the same position as the haem propionate groups (Martin *et al.*, 2010). Taken together, our molecular modelling data support the observation that gemfibrozil could bind inside the haem-binding cavity of *h*HNOX domain and that two ligand molecules could occupy simultaneously a major portion of the space occupied by cinaciguat (Supporting Information Fig. S3). Future analysis will test the involvement of these residues in gemfibrozil-dependent sGC activation. Based on distinct abilities of ataciguat and cinaciguat to protect sGC from degradation caused by haem oxidation, it has been suggested that these two molecules may have distinct binding sites (Hoffmann *et al.*, 2009). Nonetheless, our studies indicate that gemfibrozil competes with both of them. Two possible gemfibrozil molecules located within the haem cavity may explain this.

We report that gemfibrozil activates sGC with an apparent EC_{50} of 94 [75–117] μM and induces vasorelaxation with an EC_{50} of 61 [37–100] μM. For hyperlipidaemic patients taking gemfibrozil, a typical treatment regimen consists of 600 mg tablets twice daily. Pharmacokinetic studies demonstrate that one 600 mg dose of gemfibrozil results in a maximal gemfibrozil plasma concentration of 70 to 120 μM, for controlled or immediate release formulations respectively (Miller and Spence, 1998). The estimated plasma half-life of gemfibrozil is 1.3 h (Miller and Spence, 1998). These pharmacokinetic parameters suggest that patients taking gemfibrozil periodically are exposed to levels of gemfibrozil that may stimulate sGC in cardiovascular system.

We also report here that above 100 μM, gemfibrozil displays antiplatelet function. In patients on a stable regimen of anticoagulant warfarin, gemfibrozil increases the risk of bleeding or even severe hypoprothrombinaemia. While the displacement of warfarin from albumin and increased prothrombin times is the accepted explanation for fibrate-warfarin drug interaction (Wells *et al.*, 1994), antiplatelet function of gemfibrozil characterized in the current study may also be an important contributor for these adverse effects.

Previous studies demonstrated that vascular sGC with oxidized or deficient haem is targeted for degradation (Meurer *et al.*, 2009), which diminishes sGC function in vasculature. It was also reported that haem-mimicking sGC activator cinaciguat protects sGC from degradation and even reactivates it (Meurer *et al.*, 2009). Hyperlipidaemia strongly correlates with elevated vascular inflammation (Libby *et al.*, 2002), which in turn is associated with a higher content of haem-deficient or haem-oxidized sGC in the vasculature (Meurer *et al.*, 2009). Because gemfibrozil is not only an antilipidaemic drug but is also a haem-independent sGC activator with affinity for dysfunctional sGC, it may alleviate the impaired sGC-dependent vasorelaxing and antiplatelet functions and protect the integrity of sGC in hyperlipidaemic inflammatory conditions.

A systematic review and meta-analyses of clinical trial of fibrates report changes in lipid profile and an overall reduction in cardiovascular and coronary events in patients taking fibrates (Jun *et al.*, 2010). However, the extent of cardiovascular benefits differs depending on the type of fibrate analysed. The FIELD (Keech *et al.*, 2005) and ACCORD-Lipid (ACCORD Study Group *et al.*, 2010) trials of fenofibrate reported improved plasma lipid levels, but found no additional benefits. The LEADER study of bezafibrate (Meade *et al.*, 2002) shows only an insignificant decrease in the risk of major cardiovascular events. On the contrary, a large Helsinki Heart Study (Frick *et al.*, 1987) and VA-HIT (Rubins *et al.*, 1999) clinical trials of gemfibrozil reported that an improved lipid profile is accompanied by clear cardiovascular benefits. A number of different factors may contribute to the higher cardiovascular preventive benefits of gemfibrozil therapy over other fibrates. Additional clinical studies are needed to determine if gemfibrozil-dependent sGC activation described in this report occur *in vivo* and explain gemfibrozil's more pronounced cardiovascular benefit in clinical trials.

In summary, we determined that the antihyperlipidaemic drug gemfibrozil acts as a NO- and haem-independent activator of sGC and exhibits vasorelaxing and antiplatelet properties. These findings suggest that cardiovascular preventive benefits of gemfibrozil may derive not only from an altered lipid profile, but also from the protection and direct activation of sGC.

Acknowledgement

This work was supported by NIH [grant HL088128] (E. M.), the American Heart Association [Grant-in-Aid 12GRNT11930007] (E. M.) and the DFG SFB 688 TP A2 and GA 1561/1-1 (both to S. G.).

Author contributions

E. M., I. G. S., S. G., A. P. and G. A. S designed the research study, performed the research, analysed the data and wrote the paper. M. S. and N. R. performed the research.

Conflict of interest

None.

References

ACCORD Study Group, Ginsberg HN, Elam MB, Lovato LC, Crouse JR 3rd, Leiter LA *et al.* (2010). Effects of combination lipid therapy in type 2 diabetes mellitus. N Engl J Med 362: 1563–1574.

Alexander SPH, Benson HE, Faccenda E, Pawson AJ, Sharman JL, Spedding M *et al.* (2013a). The Concise Guide to PHARMACOLOGY 2013/14: Nuclear hormone receptors. Br J Pharmacol 170: 1652–1675.

Alexander SPH, Benson HE, Faccenda E, Pawson AJ, Sharman JL, Spedding M *et al.* (2013b). The Concise Guide to PHARMACOLOGY 2013/14: Enzymes. Br J Pharmacol 170: 1797–1867.

Case DA, Cheatham TE 3rd, Darden T, Gohlke H, Luo R, Merz KM Jr *et al.* (2005). The Amber biomolecular simulation programs. J Comput Chem 26: 1668–1688.

Chinetti-Gbaguidi G, Fruchart JC, Staels B (2005). Pleiotropic effects of fibrates. Curr Atheroscler Rep 7: 396–401.

Chrominski M, Banach L, Karczewski M, ó Proinsias K, Sharina I, Gryko D *et al.* (2013). Synthesis and evaluation of bifunctional sGC regulators: optimization of a connecting linker. J Med Chem 56: 7260–7277.

Ehret GB, Munroe PB, Rice KM, Bochud M, Johnson AD, Chasman DI *et al.* (2011). Genetic variants in novel pathways influence blood pressure and cardiovascular disease risk. Nature 478: 103–109.

Erdmann E, Semigran MJ, Nieminen MS, Gheorghiade M, Agrawal R, Mitrovic V *et al.* (2013a). Cinaciguat, a soluble guanylate cyclase activator, unloads the heart but also causes hypotension in acute decompensated heart failure. Eur Heart J 34: 57–67.

Erdmann J, Stark K, Esslinger UB, Rumpf PM, Koesling D, de Wit C *et al.* (2013b). Dysfunctional nitric oxide signalling increases risk of myocardial infarction. Nature 504 (7480): 432–436.

Fiser A, Sali A (2003). Modeller: generation and refinement of homology-based protein structure models. Methods Enzymol 374: 461–491.

Foerster J, Harteneck C, Malkewitz J, Schultz G, Koesling D (1996). A functional heme-binding site of soluble guanylyl cyclase requires intact N-termini of alpha 1 and beta 1 subunits. Eur J Biochem 240: 380–386.

Frick MH, Elo O, Haapa K, Heinonen OP, Heinsalmi P, Helo P *et al.* (1987). Helsinki Heart Study: primary-prevention trial with gemfibrozil in middle-aged men with dyslipidemia. Safety of treatment, changes in risk factors, and incidence of coronary heart disease. N Engl J Med 317: 1237–1245.

Fruchart JC, Duriez P (2006). Mode of action of fibrates in the regulation of triglyceride and HDL-cholesterol metabolism. Drugs Today (Barc) 42: 39–64.

Gambaryan S, Kobsar A, Rukoyatkina N, Herterich S, Geiger J, Smolenski A *et al.* (2010). Thrombin and collagen induce a feedback inhibitory signaling pathway in platelets involving dissociation of the catalytic subunit of protein kinase A from an NFkappaB-IkappaB complex. J Biol Chem 285: 18352–18363.

Herve D, Philippi A, Belbouab R, Zerah M, Chabrier S, Collardeau-Frachon S *et al.* (2014). Loss of alpha1beta1 soluble guanylate cyclase, the major nitric oxide receptor, leads to moyamoya and achalasia. Am J Hum Genet 94: 385–394.

Hoffmann LS, Schmidt PM, Keim Y, Schaefer S, Schmidt HH, Stasch JP (2009). Distinct molecular requirements for activation or stabilization of soluble guanylyl cyclase upon haem oxidation-induced degradation. Br J Pharmacol 157: 781–795.

Huey R, Morris GM, Olson AJ, Goodsell DS (2007). A semiempirical free energy force field with charge-based desolvation. J Comput Chem 28: 1145–1152.

Jun M, Foote C, Lv J, Neal B, Patel A, Nicholls SJ *et al.* (2010). Effects of fibrates on cardiovascular outcomes: a systematic review and meta-analysis. Lancet 375: 1875–1884.

Keech A, Simes RJ, Barter P, Best J, Scott R, Taskinen MR *et al.* (2005). Effects of long-term fenofibrate therapy on cardiovascular events in 9795 people with type 2 diabetes mellitus (the FIELD study): randomised controlled trial. Lancet 366: 1849–1861.

Kilkenny C, Browne W, Cuthill IC, Emerson M, Altman DG (2010). Animal research: Reporting *in vivo* experiments: the ARRIVE guidelines. Br J Pharmacol 160: 1577–1579.

Kloss S, Bouloumie A, Mulsch A (2000). Aging and chronic hypertension decrease expression of rat aortic soluble guanylyl cyclase. Hypertension 35 (1 Pt 1): 43–47.

Libby P, Ridker PM, Maseri A (2002). Inflammation and atherosclerosis. Circulation 105: 1135–1143.

Lu X, Wang L, Chen S, He L, Yang X, Shi Y *et al.* (2012). Genome-wide association study in Han Chinese identifies four new susceptibility loci for coronary artery disease. Nat Genet 44: 890–894.

Ma X, Sayed N, Beuve A, van den Akker F (2007). NO and CO differentially activate soluble guanylyl cyclase via a heme pivot-bend mechanism. EMBO J 26: 578–588.

Martin E, Lee YC, Murad F (2001). YC-1 activation of human soluble guanylyl cyclase has both heme-dependent and heme-independent components. Proc Natl Acad Sci U S A 98: 12938–12942.

Martin E, Sharina I, Kots A, Murad F (2003). A constitutively activated mutant of human soluble guanylyl cyclase (sGC): implication for the mechanism of sGC activation. Proc Natl Acad Sci U S A 100: 9208–9213.

Martin E, Golunski E, Laing ST, Estrera A, Sharina IG (2014). Alternative splicing impairs sGC function in aortic aneurysm. Am J Physiol Heart Circ Physiol 307 (11): H1565–H1575.

Martin F, Baskaran P, Ma X, Dunten PW, Schaefer M, Stasch JP *et al.* (2010). Structure of cinaciguat (BAY 58–2667) bound to Nostoc H-NOX domain reveals insights into heme-mimetic activation of the soluble guanylyl cyclase. J Biol Chem 285: 22651–22657.

McGrath J, Drummond G, McLachlan E, Kilkenny C, Wainwright C (2010). Guidelines for reporting experiments involving animals: the ARRIVE guidelines. Br J Pharmacol 160: 1573–1576.

Meade T, Zuhrie R, Cook C, Cooper J (2002). Bezafibrate in men with lower extremity arterial disease: randomised controlled trial. BMJ 325: 1139.

Meurer S, Pioch S, Pabst T, Opitz N, Schmidt PM, Beckhaus T *et al.* (2009). Nitric oxide-independent vasodilator rescues heme-oxidized soluble guanylate cyclase from proteasomal degradation. Circ Res 105: 33–41.

Miller DB, Spence JD (1998). Clinical pharmacokinetics of fibric acid derivatives (fibrates). Clin Pharmacokinet 34: 155–162.

Mindukshev I, Gambaryan S, Kehrer L, Schuetz C, Kobsar A, Rukoyatkina N *et al.* (2011). Low angle light scattering analysis: a novel quantitative method for functional characterization of human and murine platelet receptors. Clin Chem Lab Med 50: 1253–1262.

Murad F (2006). Shattuck Lecture. Nitric oxide and cyclic GMP in cell signaling and drug development. N Engl J Med 355: 2003–2011.

Pawson AJ, Sharman JL, Benson HE, Faccenda E, Alexander SP, Buneman OP *et al.*; NC-IUPHAR (2014). The IUPHAR/BPS Guide to PHARMACOLOGY: an expert-driven knowledgebase of drug targets and their ligands. Nucl. Acids Res. 42 (Database Issue): D1098–D1106.

Rubins HB, Robins SJ, Collins D, Fye CL, Anderson JW, Elam MB *et al.* (1999). Gemfibrozil for the secondary prevention of coronary heart disease in men with low levels of high-density lipoprotein cholesterol. Veterans Affairs High-Density Lipoprotein Cholesterol Intervention Trial Study Group. N Engl J Med 341: 410–418.

Ruetten H, Zabel U, Linz W, Schmidt HH (1999). Downregulation of soluble guanylyl cyclase in young and aging spontaneously hypertensive rats. Circ Res 85: 534–541.

Schmidt HH, Schmidt PM, Stasch JP (2009). NO- and haem-independent soluble guanylate cyclase activators. Handb Exp Pharmacol 191: 309–339.

Schmidt PM, Schramm M, Schroder H, Wunder F, Stasch JP (2004). Identification of residues crucially involved in the binding of the heme moiety of soluble guanylate cyclase. J Biol Chem 279: 3025–3032.

Schultz G (1974). General principles of assays for adenylate cyclase and guanylate cyclase activity. Methods Enzymol 38: 115–125.

Sharina I, Sobolevsky M, Doursout MF, Gryko D, Martin E (2011a). Cobinamides are novel co-activators of NO receptor which target sGC catalytic domain. J Pharmacol Exp Ther 340: 723–732.

Sharina IG, Jelen F, Bogatenkova EP, Thomas A, Martin E, Murad F (2008). Alpha1 soluble guanylyl cyclase (sGC) splice forms as potential regulators of human sGC activity. J Biol Chem 283: 15104–15113.

Sharina IG, Cote GJ, Martin E, Doursout MF, Murad F (2011b). RNA splicing in regulation of nitric oxide receptor soluble guanylyl cyclase. Nitric Oxide 25: 265–274.

Staels B, Dallongeville J, Auwerx J, Schoonjans K, Leitersdorf E, Fruchart JC (1998). Mechanism of action of fibrates on lipid and lipoprotein metabolism. Circulation 98: 2088–2093.

Stasch JP, Evgenov OV (2013). Soluble guanylate cyclase stimulators in pulmonary hypertension. Handb Exp Pharmacol 218: 279–313.

Stasch JP, Hobbs AJ (2009). NO-independent, haem-dependent soluble guanylate cyclase stimulators. Handb Exp Pharmacol 191: 277–308.

Vita JA (2011). Endothelial function. Circulation 124: e906–e912.

Wells PS, Holbrook AM, Crowther NR, Hirsh J (1994). Interactions of warfarin with drugs and food. Ann Intern Med 121: 676–683.

Xu J, Zou MH (2009). Molecular insights and therapeutic targets for diabetic endothelial dysfunction. Circulation 120: 1266–1286.

Zamani P, Greenberg BH (2013). Novel vasodilators in heart failure. Curr Heart Fail Rep 10: 1–11.

Supporting information

Additional Supporting Information may be found in the online version of this article at the publisher's web-site:

http://dx.doi.org/10.1111/bph.13055

Figure S1 (A) Homology model of *h*HNOX complex with cinaciguat (BAY58- 2667, orange sticks) showing His105 and the YxSxR motif residues Tyr135, Ser137, Arg139 (cyan sticks). (B) Superposition of the residues that comprise the heme-binding pocket of *Ns*HNOX (orange sticks) and *h*HNOX (cyan sticks), highlighting only those that differ. Residue numbering is shown for *Ns*HNOX/*h*HNOX respectively. Atom colours are blue for N, red for O and yellow for sulfur. (C) Alignment of human *β1* H-NOX domain (Q02153) with the *Nostoc sp* H-NOX showing 34.6% sequence identity (63/182 residues highlighted in boldface letters).
Figure S2 Quality assessment results for the model of *h*HNOX (A) and the energy-minimized model of *h*HNOX–cinaciguat complex (B). The Ramachandran plots on the left-side panels and the assessment reports on the right-side panels were calculated using the Structural Analysis and Verification Server version 3 (http://nihserver.mbi.ucla.edu/SAVES_3/). The overall quality of the energy-minimized *h*HNOX model (B) is considerably higher with respect to the initial *h*HNOX model (A), albeit the PROCHECK report (error #3) that identified two additional leucine residues in unfavorable side-chain conformations.
Figure S3 Superposition of cinaciguat (cyan carbons) with the two predicted gemfibrozil (orange carbons) poses that could mimic its crystallographic bound conformation. The designated binding site #1 is occupied by the top-ranked pose of gemfibrozil and site #2 by the third conformational cluster (Supporting Information Table S2).
Table S1 Compounds for structure-activity studies.
Table S2 The top five conformational clusters from docking of cinaciguat to the energy-minimized model of *h*HNOX.
Table S3 Results of docking gemfibrozil to the energy-minimized model of *h*HNOX.